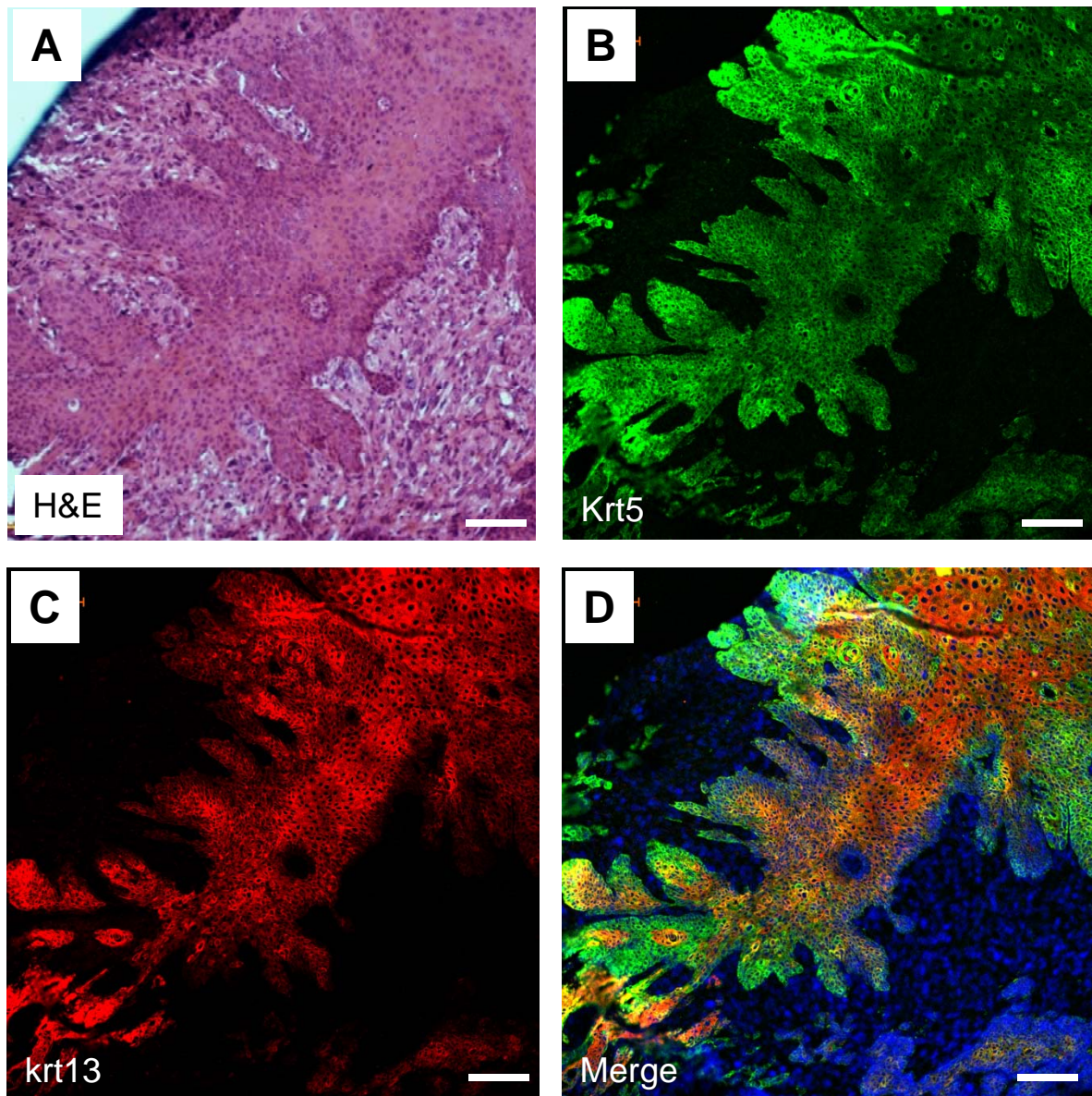
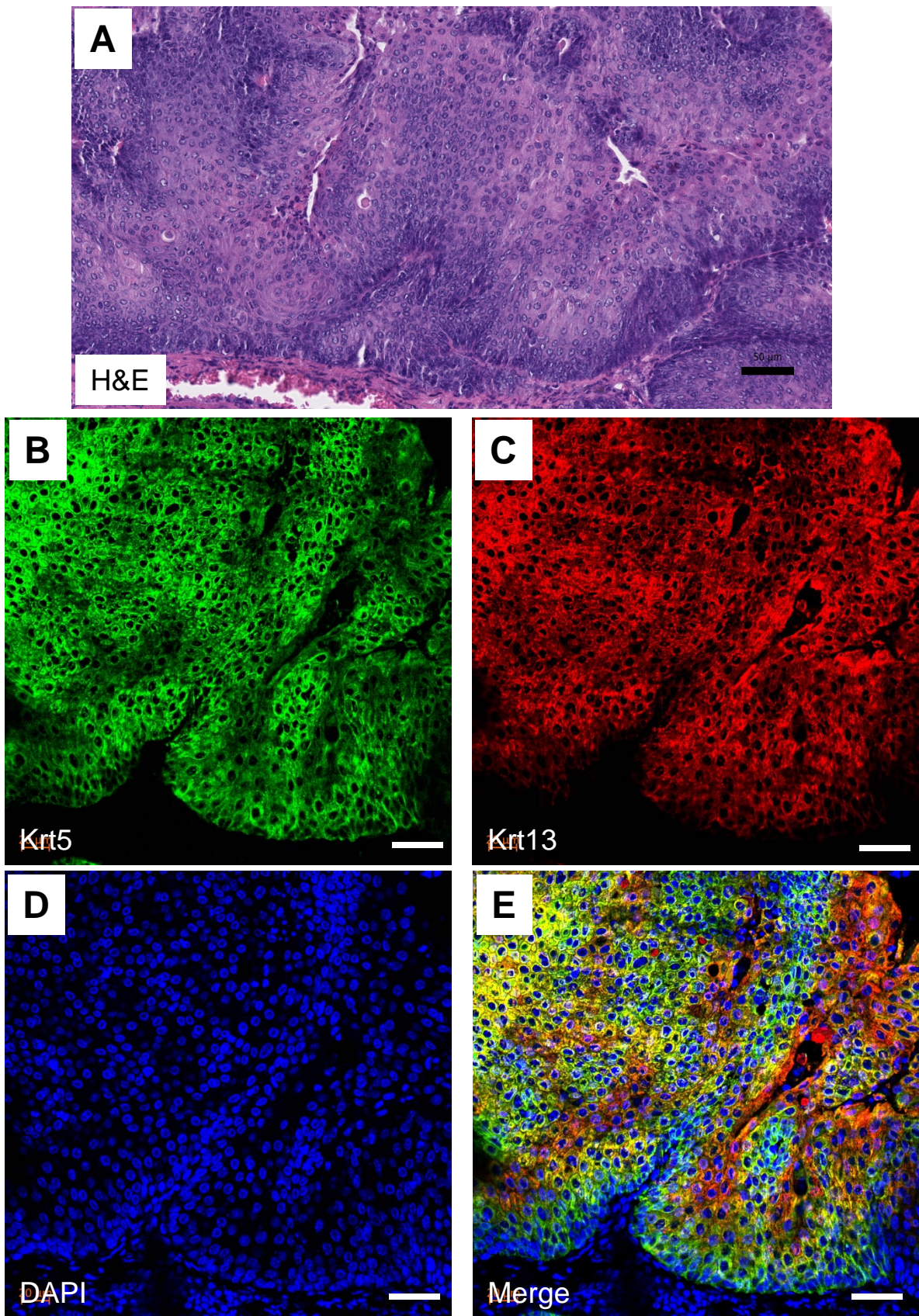


**Supplementary Figure 1.** Effects of heterozygous loss of PTEN or p53 in the absence of the other gene on urothelial proliferation assessed by histology (A & B) and anti-Krt5 immunohistochemistry (C & D). Note that heterozygous loss of PTEN does not enhance urothelial proliferation in urothelial cells lacking p53 (left column), and that heterozygous loss of p53 does not enhance PTEN loss-induced urothelial hyperplasia (right column). The scale bars equal to 50  $\mu$ m.

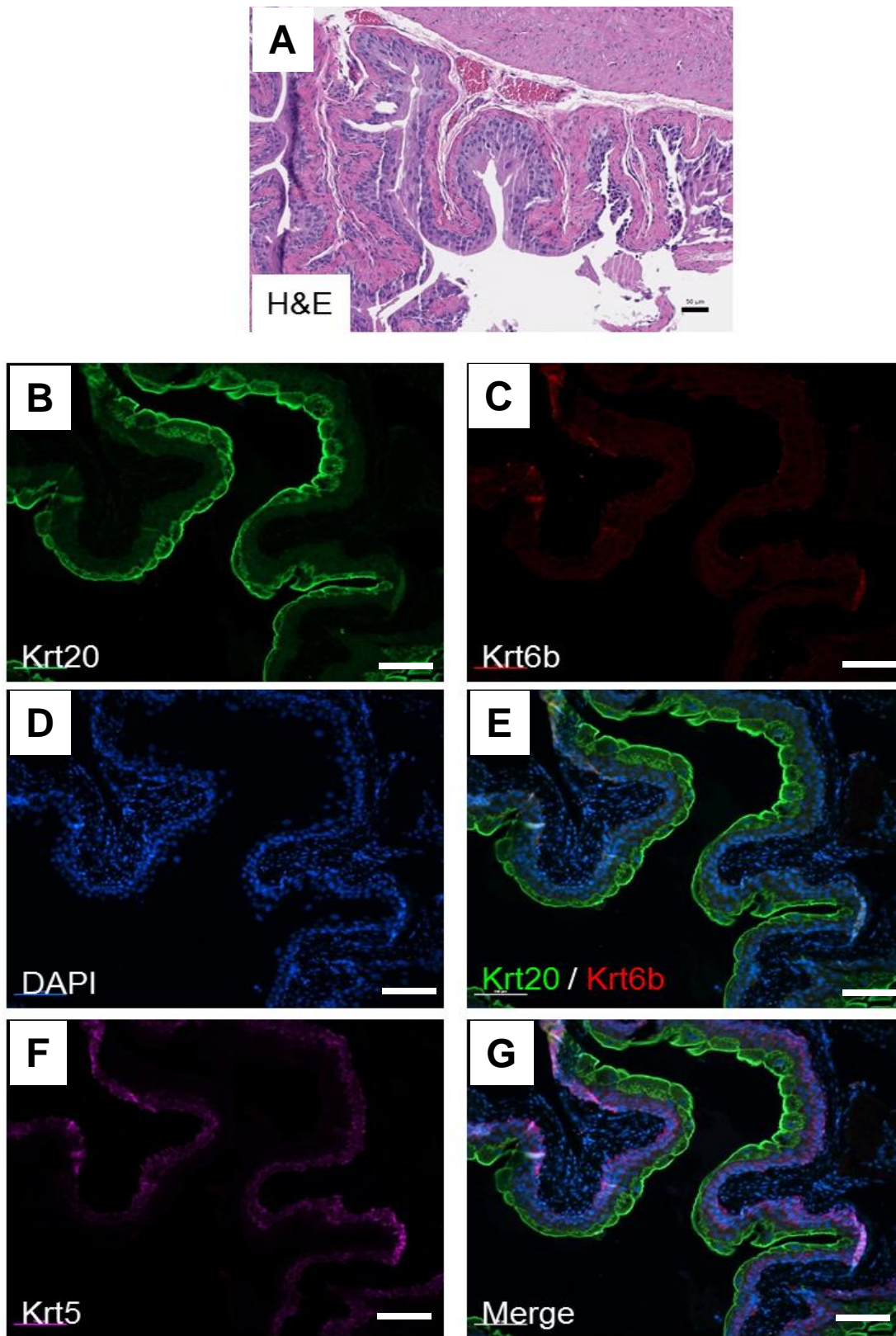


**Supplementary Figure 2.** Morphological and immunohistological features of squamous differentiation in mice lacking both Tp53 and Pten. (A) H&E of muscle-invasive lesions with overt squamous differentiation. (B & C) Strong expression of basal-cell marker Krt5 and squamous differentiation marker Krt13 in the muscle-invasive lesions. (D) Merged images exhibiting significant overlap between Krt5 and Krt13, with the former being more basal-located. The scale bars equal to 50  $\mu\text{m}$ .



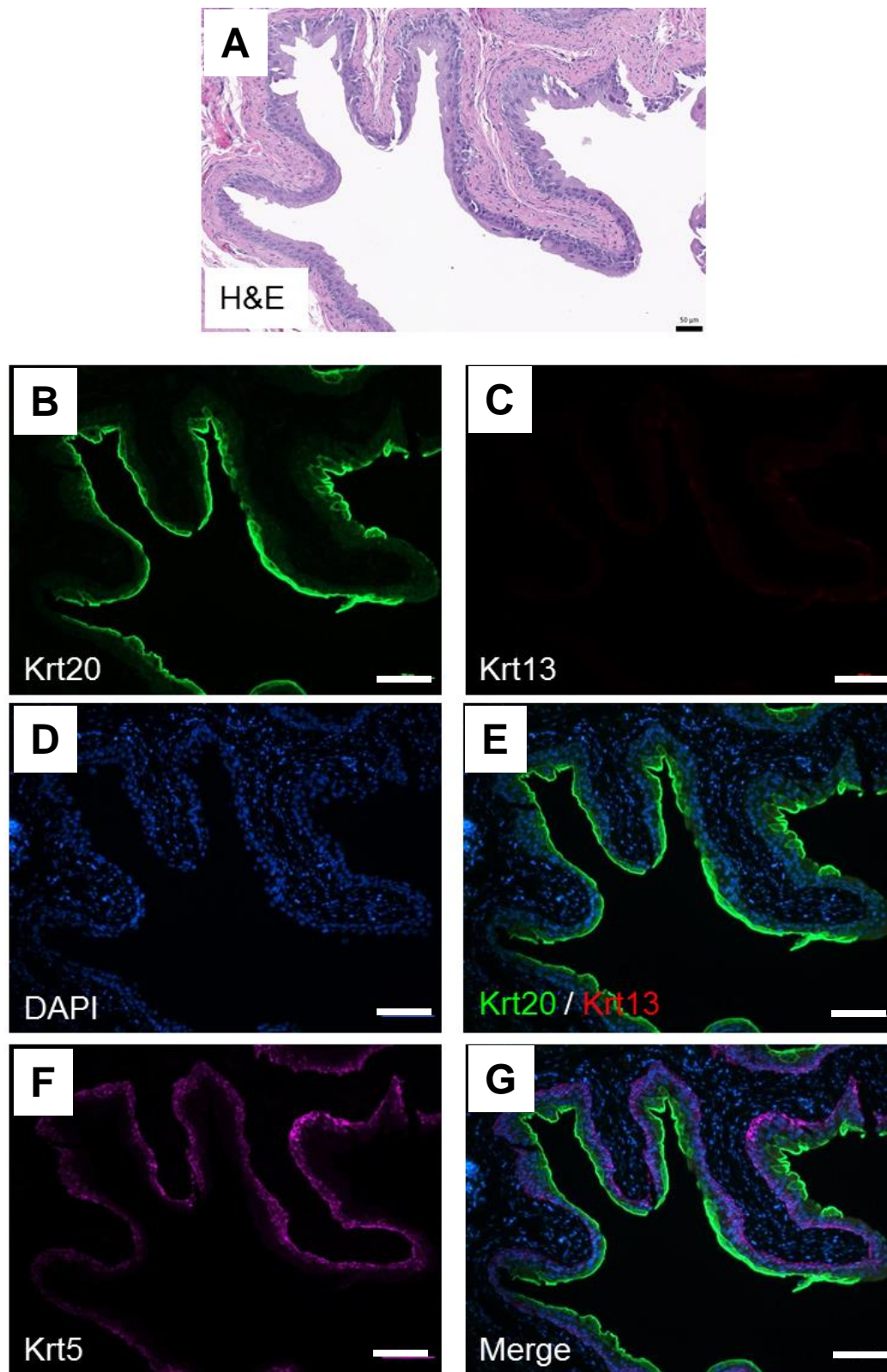
**Supplementary Figure 3.** Morphology and immunohistochemistry of additional squamous-appearing lesions in mice lacking both Tp53 and Pten. (A) H&E. (B & C) Staining with anti-Krt5 and anti-Krt13. (D) Nuclear counterstaining by DAPI. (E) Merged images. Note the strong expression of both Krt5 and Krt13 in the invasive lesions. The scale bars equal to 50 μm.

### Supplementary Fig. 3



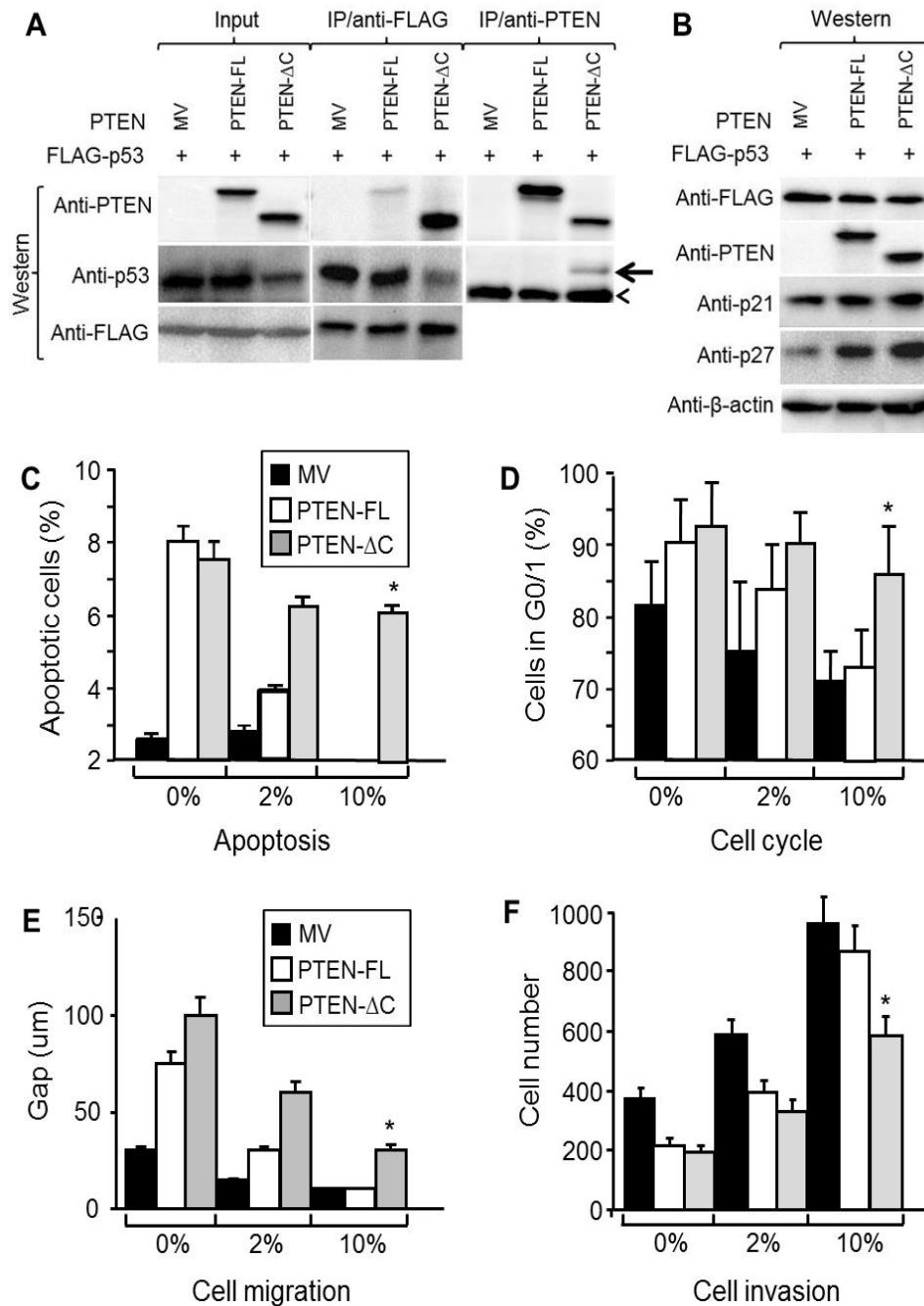
**Supplementary Figure 4.** Immunofluorescence staining of wild-type mouse urothelium using an antibody against squamous differentiation marker, Krt6b. (A) H&E staining. (B), (C) and (F) were anti-Krt20, anti-Krt6b and DAPI counter-staining, respectively. (E) and (G) were merged images. Note that, while the urothelium was labeled positively with anti-Krt20 at the luminal surface (B) and with anti-Krt5 (F) at the basal layer, it was not labeled with anti-Krt6b (C). The scale bar equals to 100 μm.

### Supplementary Fig. 4

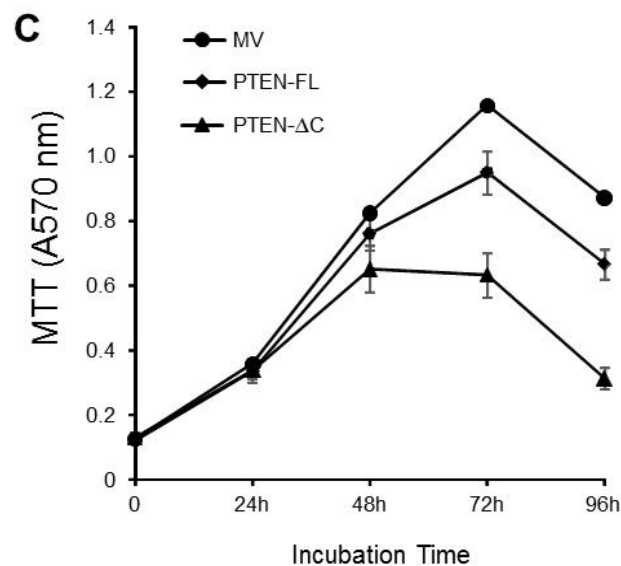
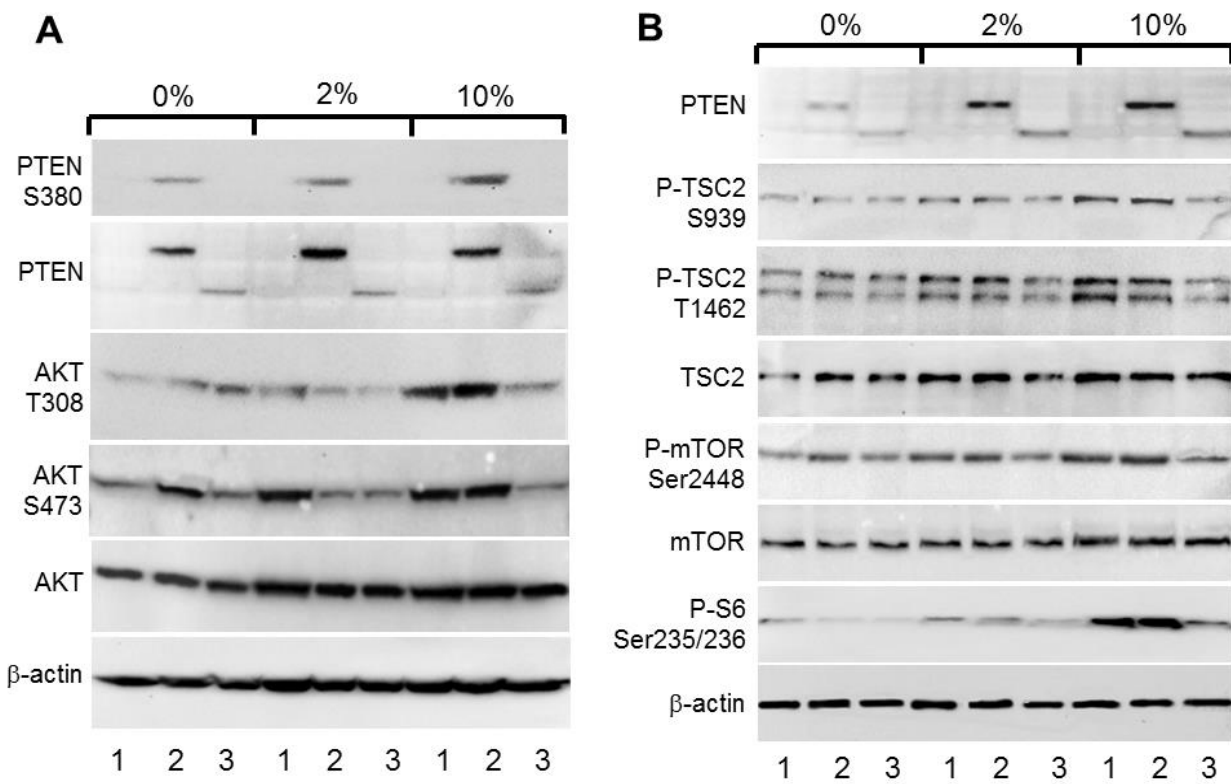


**Supplementary Figure 5.** Immunofluorescence staining of wild-type mouse urothelium (A) using an antibody against squamous differentiation marker, Krt13 (C). Note that, while the urothelium was labeled positively with anti-Krt20 at the luminal surface (B & E) and with anti-Krt5 at the basal layer (F & G), it was not labeled with anti-Krt13 (C & E). The scale bar equals to 100 μm.

**Supplementary Fig. 5**



**Supplementary Figure 6.** Co-immunoprecipitation of PTEN and p53 (A), p53 pathway status (B), and effects of stable expression of full-length and tailless PTEN on apoptosis, cell cycle progression, migration and invasion (C-F). (A) UMUC3 cells stably expressing mock vector (MV), full-length PTEN (PTEN-FL) or tailless PTEN (PTEN-TL) were secondarily transfected with FLAG-tagged p53. Immunoprecipitation was performed using anti-FLAG antibody followed by Western blotting using anti-PTEN, anti-p53 and anti-FLAG. Additionally, reverse immunoprecipitation was performed using anti-PTEN antibody followed Western blotting using anti-PTEN and anti-p53. Note that PTEN and p53 co-immunoprecipitated, much more so with the tailless PTEN. Arrow in the right panel of (A) denotes the p53 band, and arrowhead marks a non-specific band present in all differently transfected cells. (B) Western blotting showing the upregulated downstream effectors p21 and p27 more so in tailless PTEN-expressing cells than in full-length-PTEN-transfected UMUC3 cells. (C-F) UMUC3 cells stably transfected with mock vector (MV), full-length PTEN (PTEN-FL) or tailless PTEN (PTEN-TL) were grown in culture media containing 0%, 2% or 10% fetal bovine serum and then subjected to apoptosis (C), cell cycle (D), migration (E) and invasion (F) assays (see Methods for details). Note that the tailless PTEN, devoid of C-terminal phosphorylation sites, induced considerably more apoptosis than full-length PTEN, particularly in culture media containing 10% fetal bovine serum (C). Also note that there were significantly more cells in G0/G1 (D), more gaps in wound repairing (E) and fewer invasive cells (F) in UMUC3 cells expressing tailless PTEN than full-length PTEN, particularly in 10% fetal bovine serum. Asterisks mark statistical significance between the tailless PTEN group and the full-length PTEN group.



**Supplementary Figure 7.** Effects of inducible expression of full-length and tailless PTEN. UMUC3 cells were first stably transfected with a plasmid containing CMV-driven reverse tetracycline transcription activator (CMV-rtTA) (lanes 1 in panels (A) and (B)). The stable cells were additionally transfected with a plasmid containing full-length PTEN or tailless PTEN under the control of tetracycline response element (TRE-PTEN-FL (lanes 2) or TRE-PTEN-TL (lanes 3)). The transfected cells were grown in media containing 0, 2 or 10% fetal bovine serum and subsequently supplemented with doxycycline. Note that the inducible expression of the tailless PTEN exhibited significantly greater inhibitory effects in 10% fetal bovine serum on AKT phosphorylation (A) and phosphorylation of downstream effectors including TSC2, mTOR, and S6 (B). Detection of none phosphorylated versions of these proteins served as controls. (C) Cell viability (MTT) assay of UMUC3 inducibly expressing the mock vector (MV), full-length PTEN (PTEN-FL) or tailless PTEN (PTEN-ΔC) in 10% fetal bovine serum at the different incubation time points. Note that the tailless PTEN exhibited stronger inhibition of cell survival than the full-length PTEN.